

Muon Dynamics in a Toroidal Sector Magnet

Juan C. Gallardo¹, Richard C. Fernow and Robert B. Palmer

Physics Department, Brookhaven National Laboratory, Upton, NY 11973, USA

Abstract. We present a Hamiltonian formulation of muon dynamics in toroidal sector solenoids (bent solenoid).

I INTRODUCTION

The present scenario for the cooling channel in a high brightness muon collider [1] calls for a quasi-continuous solenoidal focusing channel. The beam line consists of a periodic array of hydrogen absorbers immersed in a solenoid with alternating focusing field and rf linacs at the zero field points.

The simple $\frac{dE}{dx}$ energy loss in conjunction with multiple scattering and energy straggling leads to a decrease of the normalized transverse emittance. Reduction of the longitudinal emittance could be achieved by wedges of material located in dispersive regions; at least in principle, this scenario seems appropriate to obtain effective 6-D phase space reduction. [2]

A conventional chicane is a dispersion element but its use presents a serious challenge, as it is very difficult to integrate it with the solenoidal channel. The matching into the periodic solenoidal system imposes constraints on the Twiss parameters of the beam which seems not easily achievable. A possible alternative is the use of curved solenoids in conjunction with wedge absorbers as suggested by one of the authors. [3]

Solenoids and toroidal sectors have a natural place in muon collider design given the large emittance of the beam and consequently, the large transverse momentum of the initial pion beam or the decay muon beam. Bent solenoids as shown in Fig.1 were studied for use at the front end of the machine, as part of the capture channel [4] and more recently as part of a diagnostic setup to measure the position and momentum of muons. [5]

¹⁾ Email:gallardo@bnl.gov

II TOROIDAL SECTOR SOLENOID

If we restrict ourselves for the moment to a horizontal bending plane, the magnetic field inside of the solenoid and near the axis has a gradient (field lines are denser at smaller radius) described approximately by $\vec{B}(x, y, s) \approx B_s \vec{e}_s$ with

$$B_s(x, y, s) \approx \frac{B_s(0, 0, s)}{(1 + hx)} \quad (1)$$

where s is the coordinate along the particle trajectory and $h = \frac{1}{R_o}$ is the curvature at the position s , with R_o the radius of curvature. As a consequence of the curvature of the trajectory and the corresponding magnetic gradient, the center of the particle guide orbit, averaged over the Larmor period, drifts in a direction perpendicular to the plane of bending [6]. The combined drift velocity can be written as,

$$\frac{d\vec{r}}{dt} = v_{\parallel} \frac{\vec{B}}{B} + \frac{m_{\mu}}{2q_{\mu}} (2v_{\parallel}^2 + v_{\perp}^2) \frac{(\vec{R}_o \times \vec{B})}{(1 + hx) R_o^2 B^2}. \quad (2)$$

and the magnitude of the transverse drift velocity is

$$v_{\text{drift}}^T = \frac{m_{\mu}}{2q_{\mu}} (2v_{\parallel}^2 + v_{\perp}^2) \frac{h}{(1 + hx) B_s} \quad (3)$$

Clearly a y-position versus energy (v_{\parallel}) correlation will develop as the muon beam travels along the toroidal sector solenoid.

From Eq.2 above we notice that if we include an additional vertical field, a dipole with a curvature equal to that of the bent solenoid for the reference energy, i.e.

$$\vec{B}_D \approx -\frac{|B|}{v_{\parallel}} v_{\text{drift}}^T \vec{e}_y \quad (4)$$

then Eq.2 reduces to,

$$\frac{d\vec{r}}{dt} = v_{\parallel} \frac{B_s}{|B|} \vec{e}_s + (v_{\parallel} - v_{\parallel}^o) \frac{B_D}{|B|} \vec{e}_y \quad (5)$$

and consequently, particles with the chosen energy will not drift vertically and will remain on the axis of the bent solenoid. Those particles with larger energy will drift upward (positive y-direction) and those with lower energy downward (negative y-direction), achieving the needed dispersion. The magnitude of the dispersion is given by

$$D_y = 2\pi \frac{p_o}{q} \frac{B_D}{B_s^2} = 2\pi h \left(\frac{p_o}{q B_s} \right)^2 \quad (6)$$

where p_o is the chosen momentum corresponding to zero dispersion.

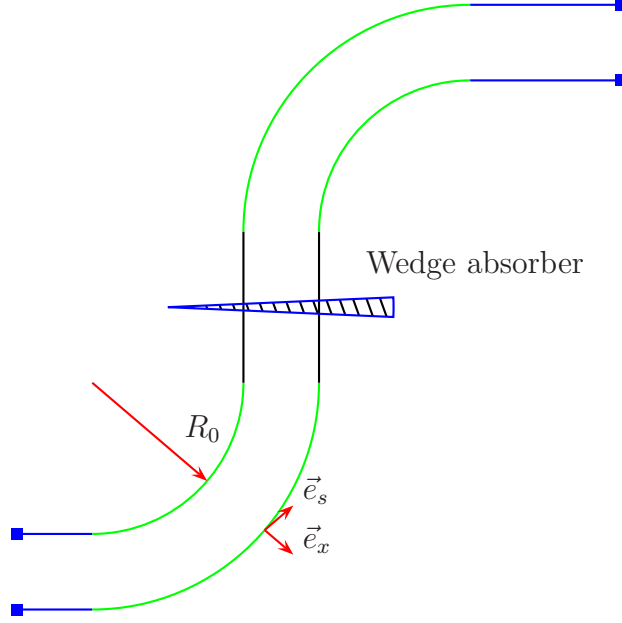


FIGURE 1. Schematic of emittance exchange system with a bent solenoid

III DYNAMICS IN A TOROIDAL SOLENOID. HAMILTONIAN FORMULATION

From general principles of classical mechanics and following the usual approximations in accelerator physics [7] the normalized Hamiltonian reads,

$$H(x, p_x, y, p_y, z, \delta; s) \approx -\frac{q}{p_0}(1 + hx)A_s(s) - (1 + \delta)hx + \frac{(1+hx)}{2(1+\delta)} \left\{ (p_x - \frac{q}{p_0}A_x)^2 + (p_y - \frac{q}{p_0}A_y)^2 \right\} \quad (7)$$

where the path length s is the independent variable, p_x, p_y are normalized momenta with respect to p_0 , the initial reference total momentum $p_0 = \sqrt{p_x^2 + p_y^2 + p_s^2}$; $z = s - \beta_o ct$, $\delta = \frac{(p-p_0)}{p_0}$ and $\vec{A} = (A_x, A_y, A_s)$ is the vector potential. The vector potential satisfies the gauge condition $\nabla \cdot \vec{A} = 0$.

In the accelerator frame of reference, i.e. the Frenet-Serret coordinate system defined by the metric,

$$d\sigma^2 = dx^2 + dy^2 + (1 + hx)^2 ds^2 \quad (8)$$

the equations for the coordinate unit vectors are

$$\frac{d\vec{e}_x}{ds} = h(s)\vec{e}_s, \quad \frac{d\vec{e}_y}{ds} = 0, \quad \frac{d\vec{e}_s}{ds} = -h(s)\vec{e}_x \quad (9)$$

The magnetic and electric fields are obtained from

$$\vec{B} = \nabla \times \vec{A} \quad \text{and} \quad \vec{E} = c\beta_0 \frac{\partial \vec{A}}{\partial z} \quad (10)$$

with

$$\begin{aligned} \nabla \times \vec{A} = & \frac{1}{(1+hx)} \{ \partial_y (1+hx) A_s - \partial_s A_y \} \vec{e}_x \\ & + \frac{1}{(1+hx)} \{ \partial_s A_x - \partial_x (1+hx) A_s \} \vec{e}_y \\ & + \{ \partial_x A_y - \partial_y A_x \} \vec{e}_s \end{aligned} \quad (11)$$

and

$$\nabla \cdot \vec{A} = \frac{1}{(1+hx)} \left[\frac{\partial}{\partial x} (A_x(1+hx)) + \frac{\partial}{\partial y} (A_y(1+hx)) + \frac{\partial}{\partial s} A_s \right] \quad (12)$$

The lowest order approximation for a toroidal solenoidal field is given by Eq.1. The corresponding vector potential in the next order is [8],

$$\vec{A} = -\frac{1}{2} B_o \frac{y}{(1+hx)} \vec{e}_x + \frac{B_o}{2h} \ln(1+hx) \vec{e}_y \quad (13)$$

and the corresponding magnetic fields are:

$$\begin{aligned} B_x = & -\frac{1}{(1+h(s)x)} \frac{1}{2h(s)} \left\{ \frac{dB_o}{ds} \ln(1+h(s)x) \right. \\ & \left. - \frac{B_o}{h(s)} h'(s) \ln(1+h(s)x) + h'(s) \frac{B_o x}{(1+h(s)x)} \right\} \end{aligned} \quad (14a)$$

$$B_y = -\frac{1}{2(1+h(s)x)^2} \left\{ \frac{dB_o}{ds} y - h'(s) \frac{B_o(s)xy}{1+h(s)x} \right\} \quad (14b)$$

$$B_s = \frac{B_o}{1+h(s)x} \quad (14c)$$

One possible second order approximation for the vector potential of a dipole is

$$A_x = -\frac{B_D}{2h(s)} \frac{h''(s) x (y^2 - \frac{1}{3}x^2)}{(1+h(s)x)} \quad (15a)$$

$$A_y = \frac{B_D}{2h(s)} \frac{h'(s) xy}{(1+h(s)x)} \quad (15b)$$

$$A_s = -\frac{B_D}{2h(s)} \left\{ 1 + h(s)x - h'(s)(y^2 - x^2) \right\} \quad (15c)$$

Substituting the total vector potential into the Hamiltonian, and dropping some constants we can write,

$$H_{\text{tor.sol.}}^{\text{dip}}(x, p_x, y, p_y, z, \delta; s) \approx \frac{1}{2}(hx)^2 - \delta hx + \frac{(1+hx)}{2(1+\delta)} \left\{ (p_x - \frac{q}{p_o} A_x)^2 + (p_y - \frac{q}{p_o} A_y)^2 \right\} \quad (16)$$

We have written a simple Fortran program to solve the equations of motion from the above Hamiltonian ; its result for a few representative cases of interest are shown in Fig.2.

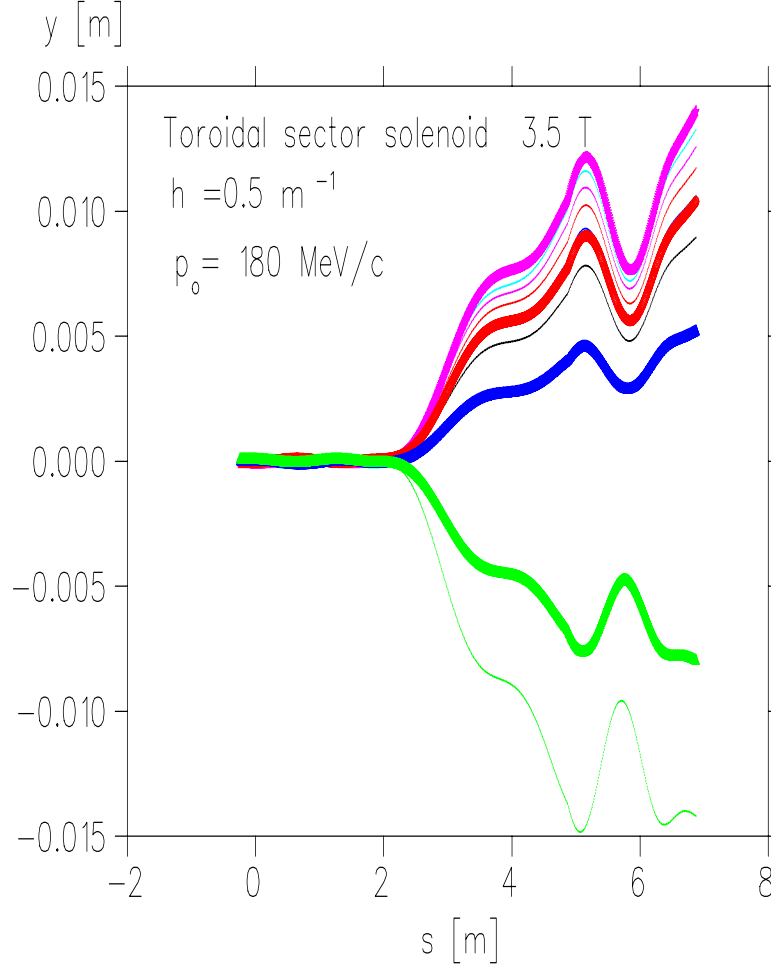


FIGURE 2. Example of dispersion created by a toroidal sector solenoid plus a vertical dipole. We show several tracks with energies ($\pm 1\%$) larger and smaller than the reference energy p_o .

A second order expansion of the bent solenoid magnetic field given in Eqs. 14 has been used together with a second order expansion of the dipole magnetic field in the cooling simulation program ICOOL [9]. Fig.3a shows an example of the dispersion D_y in a bent solenoid obtained in ICOOL as a function of the dipole strength B_D . It is apparent that the dependence of Eq. 6 on B_D is well satisfied. Likewise, Fig 3b shows simulation results for the dispersion as a function of B_s^{-2} . Again we see that the mentioned equation gives a good representation of the results.

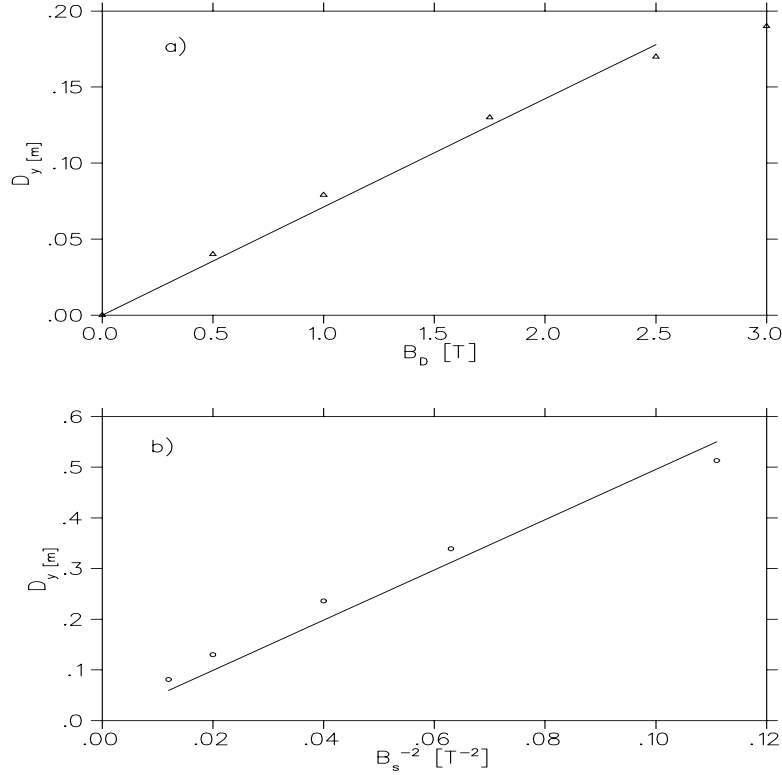


FIGURE 3. a) Dispersion, D_y vs. dipole magnetic field, B_D ; b) Dispersion, D_y vs. solenoid magnetic field B_s^{-2} .

IV ACKNOWLEDGEMENTS

This work was supported by the US DoE under Contract No. DE-AC02-76CH00016.

REFERENCES

1. R. B. Palmer, presentation at FNAL Muon Collider Collaboration Meeting, July 1995, unpublished; R. B. Palmer, et al., *Muon Colliders*, 9th Advanced ICFA Beam Dynamics Workshop, Ed. Juan C. Gallardo, AIP Press, AIP Conference Proceedings 372, (1996).
2. R. B. Palmer, *Cooling Theory*, in preparation.
3. R. B. Palmer, private communication.
4. $\mu^+\mu^-$ Collider: A Feasibility Study, New Directions for High-Energy Physics. Proceedings of the 1996 DPF/DPB Summer Study on High-Energy Physics Snowmass'96, Chapter 4; see also the Muon Collider Collaboration WEB page <http://www.cap.bnl.gov/mumu/>

5. C. Lu, K. T. McDonald and E. J. Prebys, *A Detector Scenario for the Muon Cooling Experiment*, Princeton/ $\mu\mu$ /97-8, July 1997.
6. F. Chen, *Introduction to Plasma Physics*, Chap.2, Plenum Press (1979).
7. C. Wang and A. Chao, *Notes on Lie algebraic analysis of achromats*, SLAC/AP-100, Jan. 1995; E. D. Courant and H. S. Snyder, *Theory of the alternating-gradient synchrotron*, Ann. of Phys. 3,1 (1958); R. Ruth, *Single Particle Dynamics in Circular Accelerators*, Physics of Particle Accelerators, AIP Conference Proc. 153, Ed. M. Month and M. Dienes, Vol.1, pag. 150, (1987); C. Wang and A. Chao, *Transfer matrices of superimposed magnets and RF cavity*, SLAC/AP-106, Nov. 1996; H. Wiedemann, *Particle Accelerator Physics II*, pag. 51, Springer (1995).
8. See C. Wang and A. Chao [7] and A. Morozov and Solov'ev, *Motion of charged particles in e.m. fields*, Review of Plasma Physics, vol. II, Ed. M. A. Leontovich, Consultants Bureau, Division of Plenum Publishing Company, New York (1966).
9. R. Fernow, ICOOL, fortran program to simulate muon ionization cooling.